$TlGa_{1-x}Er_xSe_2$ SOLID SOLUTIONS, THEIR ELECTRICAL AND OPTICAL PROPERTIES

E.M. KERIMOVA, S.N. MUSTAFAEVA, N.Z. GASANOV, K.M. HUSEYNOVA, Q.M. SHARIFOV

Institute of Physics, National Academy of Sciences of Azerbaijan, Baku, AZ-1143
*e-mail: *ngasanov@yandex.ru*

The complex permittivity, dielectric loss tangent, and conductivity σ_{ac} of $TlGa_{1-x}Er_xSe_2$ solid solutions (x = 0; 0.001; 0.005) were studied in the temperature range 150-300 K in an alternating electric field (25-10^6 Hz). The change in dielectric constant as a function of temperature in the studied crystals is due to the presence of low-frequency relaxation polarization. Conductivity obeys the law $\sigma_{ac} \sim f^{0.8}$ at frequencies of 10^2–10^4 Hz, which, in the studied crystals, indicates the presence of hopping conductivity by states localized near the Fermi level. The parameters of the states localized in the $TlGa_{1-x}Er_xSe_2$ band gap are estimated. It was shown that an increase in the Er impurity leads to an increase in the density of localized states in $TlGaSe_2$ and a decrease in their energy spread. The optical absorption edge of $TlGa_{1-x}Er_xSe_2$ crystals was studied, and the temperature dependence of the band gap in them was obtained.

Keywords: solid solutions, complex dielectric permittivity, frequency dispersion, dielectric loss, conductivity, optical absorption edge.
PACS: 72.20.-i ; 78.00.00

1. INTRODUCTION

$TlGaSe_2$ crystal has a layered structure of $A^{III}B^{III}C^{VI}_2$ thallium chalcogenide type compounds. This crystal has a monoclinic structure, $C2/c\text{-}C^6_{2h}$ space group, with unit cell parameters a =10.772, b =10.771, c =15.636, β =100.6° [1].

$TlGaSe_2$ is a p-type wide-gap semiconductor and possesses practically important physical characteristics: high photo- and X-ray sensitivity. On its basis, photoelectric converters, spectrum analyzers, X-ray, gamma, and neutron detectors [2,3,4] are developed, and the possibility of creating a phototransistor is shown [5].

In [6,7], hopping conductivity in $TlGaSe_2$ single crystals was studied. The results of studying the effect of γ radiation on the conductivity and dielectric characteristics of $TlGaSe_2$ single crystals are presented in [8,9]. Many works, for example [10,11], are devoted to the study of the optical properties of the $TlGaSe_2$ compound.

Specific feature of $A^{III}B^{III}C^{VI}_2$ family crystals is that these semiconductors also possess ferroelectric properties. Due to the layered structure, polytypic modifications occur, resulting in changes in their physical properties [12]. In addition, a large number of crystals of this type are characterized by consecutive phase transitions[13,14].

Our assessment of the solubility of erbium in the $TlGaSe_2$ lattice, taking into account the known effective ionic atomic radii, indicates that the radius of the implanted Er^{3+} impurity atom (1.03Å) is closer to the Ga^{3+} radius (0.76Å) than to the Tl^{1+} radius (1.64Å), i.e. the partial replacement of gallium with erbium in layered $TlGaSe_2$ crystals corresponds to the condition for the formation of a substitution solution. The aim of this work is to study the electrical, dielectric, and optical properties of $TlGa_{1-x}Er_xSe_2$ solid solutions (x = 0; 0.001; 0.005).

2. METHODS OF THE INVESTIGATION

The synthesis of $TlGa_{1-x}Er_xSe_2$ solid solutions (x =0; 0.001; 0.005) was carried out by fusing highly pure chemical elements taken in stoichiometric ratios in quartz ampoules evacuated to 10^{-3} Pa. Samples were homogenized by annealing at a temperature of 750K for 120h. Single crystals of $TlGa_{1-x}Er_xSe_2$ were grown from the synthesized compounds by the Bridgman method [15]. The crystals were layered and easily chipped along the basic plane. X-ray phase analysis of the obtained samples was carried out on a D8-ADVANCE diffractometer in the mode 0.5°<2θ<80° (CuKα radiation, λ=1.5418Å).

The dielectric constant ε and the dielectric loss tangent $tan\delta$ were measured using the capacitor method in the temperature range 150-300 K using an E7-25 digital device on single-crystal wafers 0.2-0.3 mm thick. The contacts were made of silver paste. The frequency range of the alternating electric field was 25-10^6 Hz.

The measurements of the capacity of the samples were carried out with an accuracy of ±0.01 pF, and the error in measuring the quality factor ($Q = 1/tan\delta$) was 0.001%.

The electrical conductivity σ was measured along the layers by the four-probe method in the mode of continuous increase (decrease) in the sample temperature at a rate of ≈ 0.1K/min. The amplitude of the alternating electric field applied to the samples was within the ohmic region of the current-voltage characteristic.

Samples for studying the optical absorption spectra of layered semiconductor crystals of $TlGa_{1-x}Er_xSe_2$ (x =0; 0.001; 0.005) were chipped from a single-crystal ingot and had the form of thin plates with a thickness of 20 to 140μm. Light was directed to the samples parallel to the crystallographic axis c. The optical transmission spectra were studied using an apparatus based on an MDR-23 monochromator and a

131, H.Javid ave, AZ-1143, Baku
ANAS, Institute of Physics
E-mail: jophphysics@gmail.com

nitrogen cryostat with temperature stabilization in the range 77–300K (stabilization accuracy ±0.5K). The resolution of the installation was 2Å.

To measure the optical absorption coefficient in a wide range from 10 to 10^4 cm^{-1}, we used the data of measurements of the intensity of the light beam passing through samples with different thicknesses, and to cover the entire interval, we had to break it into 3 sections and take into account the transmission measurements of three pairs of samples of corresponding thicknesses for each composition studied. For each plot, the absorption coefficient was calculated by the formula $\alpha = 1/(d_2 - d_1)\ln(I_1/I_2)$, where d_1 and d_2 are the thicknesses of the samples, and I_1 and I_2 are the intensities of the light transmitted through them. Since the value of αd was greater than unity for each sample and the corresponding section, the interference of light beams passing through and reflected from the back plane of the crystal plate was very weak, and we did not observe it.

3. EXPERIMENT RESULTS AND DISCUSSION

When processing X-ray data of $TlGa_{1-x}Er_xSe_2$ solid solutions, it was found that the amount of Er impurity element used (x = 0.001; 0.005) has little effect on the lattice parameters of the initial $TlGaSe_2$ compound. However, the addition of Er to $TlGaSe_2$ leads to a change in the color of the initial crystal to a darker one (see Fig.1).

The results of X-ray analysis of the crystals under study are presented in Tables 1, 2 and 3. X-ray studies showed that $TlGa_{1-x}Er_xSe_2$ (x = 0; 0.001; 0.005) single crystals have a monoclinic structure, space group C_s^4, and the following lattice parameters were obtained: a =10.744 Å, b = 10.773Å, **c** = 15.623 Å, β =100.04°, z=16, which is in good agreement with [1]. The frequency dependences of the conductivity of $TlGa_{1-x}Er_xSe_2$ crystals at room temperature are shown in the Fig.2.

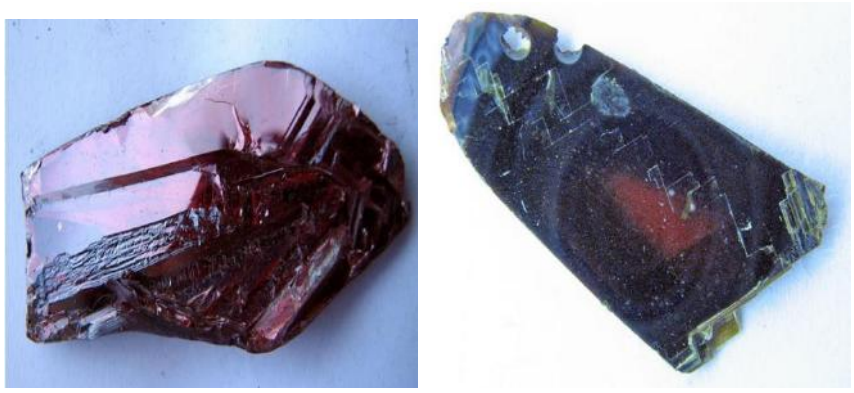

Fig. 1. Single crystals grown by the Bridgman method: $TlGaSe_2$ on the left, $TlGa_{0.995}Er_{0.005}Se_2$ on the right.

Table 1.

Calculation of the X-ray diffraction pattern of the $TlGa_{0,999}Er_{0,001}Se_2$ crystal.

№	2θ	I/I_0, %	d_{exp}(Å)	d_{calc}(Å)	hkl
1	11º46'	17,4	7,715	7,695	200
2	23º11'	100	3,845	3,878	422
3	23º6'	8,1	3,767	3,778	122
4	24º95'	2,8	3,566	2,568	222
5	26º30'	2	3,386	2,398	031
6	27º54'	6,4	3,236	2,236	322
7	31º09'	18,9	2,875	2,878	422
8	33º82'	2,9	2,648	2,650	140
9	34º97'	31,8	2,564	2,544	522
10	37º80'	2,1	2,378	2,382	404
11	47º26'	7,7	1,922	1,924	215
12	47º80'	5,8	1,901	1,902	144
13	53º84'	2,8	1,702	1,703	740
14	56º27'	2	1,634	1,634	831
15	58º13'	2,1	1,586	1,587	362

Table 2.

Calculation of the X-ray diffraction pattern of the $TlGa_{0,995}Er_{0,005}Se_2$ crystal.

№	2θ	I/I_0, %	d_{exp}(Å)	d_{calc}(Å)	hkl
1	11°44'	13,8	7,726	7,625	200
2	23°11'	100	3,846	3,847	400
3	23°52'	8,3	3,779	3,777	122
4	24°98'	2,4	3,562	2,568	222
5	26°33'	2,5	3,382	2,392	031
6	27°54'	6,4	3,237	2,237	322
7	31°05'	18,5	2,878	2,878	422
8	33°83'	4	2,648	2,650	140
9	35°01'	43,1	2,561	2,565	600
10	35°40'	2,5	2,534	2,544	522
11	41°42'	1,8	2,178	2,185	711
12	47°25'	7,9	1,922	1,923	802
13	47°81'	5	1,901	1,902	144
14	50°52'	1,6	1,805	1,806	153
15	53°88'	3,4	1,700	1,702	740
16	56°18'	1,9	1,636	1,634	426
17	58°15'	1,9	1,585	1,587	362
18	64°14'	1,4	1,451	1,437	835
19	65°05'	1,8	1,433	1,433	264

Table 3.

Crystal lattice parameters of solid solutions of the $TlGaSe_2$-$TlErSe_2$ system.

Compound	Crystal lattice system	Crystal lattice parameters, (Å)			The number of formula units in a unit cell, Z
		a	***b***	***c***	
$TlGa_{0,999}Er_{0,001}Se_2$	monoclinic	10,744	10,773	15,623	16
$TlGa_{0,995}Er_{0,005}Se_2$	monoclinic	10,744	10,773	15,623	16
$TlGaSe_2$	monoclinic	10,715	10,694	15,690	16

Table 4.

The parameters of localized states in $TlGa_{1-x}Er_xSe_2$ solid solutions obtained from high-frequency dielectric measurements.

Crystal composition $TlGa_{1-x}Er_xSe_2$	T, K	N_F, $eV^{-1}cm^{-3}$	ΔE, meV	N_t, cm^{-3}
x = 0	180	$1.54 \cdot 10^{18}$	10	$1.54 \cdot 10^{16}$
	230	$1.76 \cdot 10^{18}$	9	$1.56 \cdot 10^{16}$
	300	$2.23 \cdot 10^{18}$	7	$1.57 \cdot 10^{16}$
x = 0.005	180	$2.48 \cdot 10^{18}$	6.7	$1.66 \cdot 10^{16}$
	230	$2.58 \cdot 10^{18}$	6.3	$1.62 \cdot 10^{16}$
	300	$3.08 \cdot 10^{18}$	5	$1.54 \cdot 10^{16}$

From this it can be seen that for compositions with 0.5% and 1% Er, the difference is small. Therefore, we studied the temperature dependences of the dielectric characteristics for the composition $TlGa_{0.995}Er_{0.005}Se_2$.

Fig. 3(a) ($TlGaSe_2$) and 3(b) (Er 0.5%) show the temperature dependence of the dielectric permittivity ε. It can be seen that, with increasing temperature, ε has a tendency to increase, especially at low frequencies.

Fig. 4 shows the temperature dependence of the electrical conductivity σ. For the $TlGa_{0.995}Er_{0.005}Se_2$ samples, as shown in the dielectric permittivity, the value of σ increases as the temperature increases. The absolute value of σ depends on the frequency of the measurement area, which is more pronounced at lower temperatures. The value of σ increases several times as the frequency increases. At low temperatures,

conductivity is practically independent of temperature. In the high temperature region, the conductivity increases exponentially with the law of $\sigma \sim e^{1/T}$. This indicates that at high temperatures σ mainly depends on the concentration of the main carriers.

Fig, 5(a) and 5(b) show the temperature dependence of the dielectric loss tangent ($tan\delta$). As can be seen from the pictures, the values of the $tan\delta$ of the $TlGa_{0.995}Er_{0.005}Se_2$ crystal increase as the temperature rises compared with $TlGaSe_2$. This increase can be related to the increased concentration of free charge carriers.

As can be seen from Fig.6, the value of the dielectric permittivity of $TlGa_{1-x}Er_xSe_2$ solid solutions decreases with increasing frequency. Such behavior of the dielectric permittivity in the studied crystals is due to the presence of low relaxation polarization at low frequencies, causing dielectric loss at low frequencies. In the $tan\delta(T)$ curves, the semiconductor maximums are visible and spread when the frequency of the measurement increases from 1kHz to 1MHz.

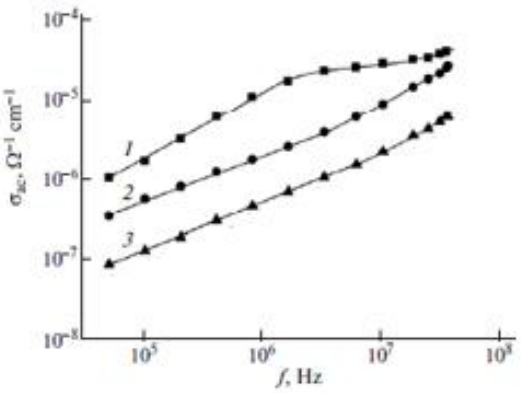

Fig. 2. Frequency dependent ac-conductivity of the $TlGa_{1-x}Er_xSe_2$ crystals: x = 0 (1), 0.001 (2), 0.005 (3). T = 300 K.

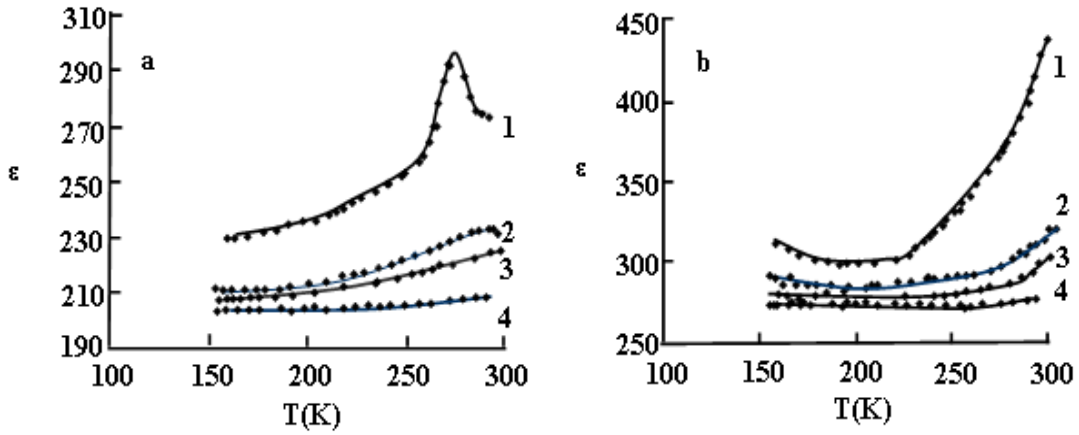

Fig. 3. Temperature dependence of dielectric permittivity of the $TlGa_{1-x}Er_xSe_2$ single crystal: a) x=0; b) x=0.005. (1- 1 kHz, 2- 10 kHz, 3- 100 kHz, 4- 1 MHz).

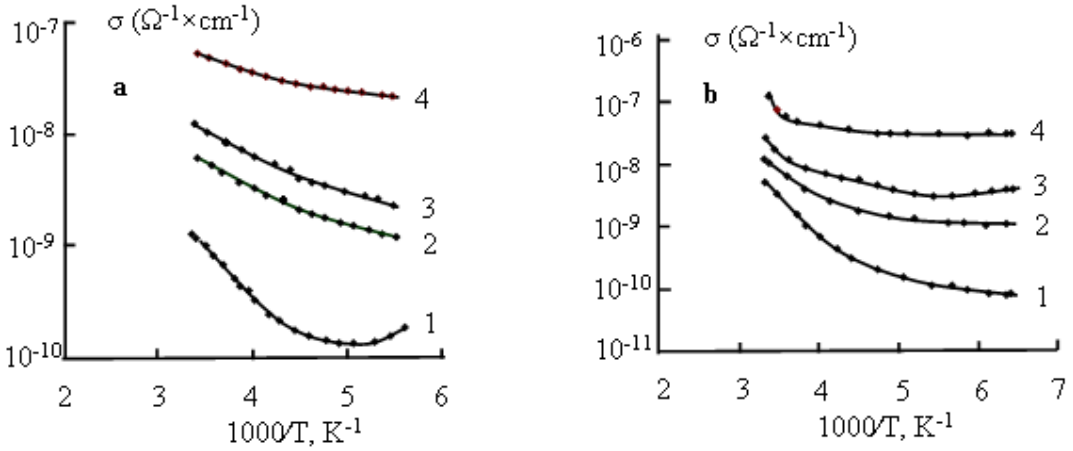

Fig. 4. Temperature dependence of the electrical conductivity of the $TlGa_{1-x}Er_xSe_2$ crystals: a) x=0; b) x=0.005. (1-1kHz, 2-10 kHz, 3-100kHz, 4-1MHz).

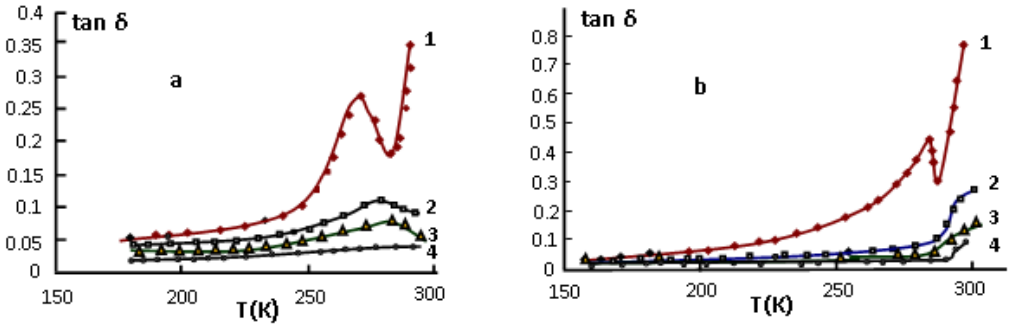

Fig. 5. Temperature dependence of the loss tangent in the $TlGa_{1-x}Er_xSe_2$ crystals:
a) x=0; b) x=0.005. (1-1kHz, 2-10 kHz, 3-100kHz, 4-1MHz).

That is, these maximums are located in the temperature region, where the value of the dielectric permittivity is sharply increased. This anomaly is due to the ferroelectric phase transition in $TlGaSe_2$, which is also due to the dimensionless phase in the temperature region [16]. The real part of dielectric permittivity (ε') decreases with increasing frequency for $TlGaSe_2$ and $TlGa_{0.995}Er_{0.005}Se_2$. The increase in temperature, as well as the impurity of 0.5% Er in the $TlGaSe_2$ crystal, significantly increases the value of the ε'.

The frequency dependence of the imaginary part ε'' of the complex dielectric permittivity of $TlGa_{1-x}Er_xSe_2$ (x=0; 0.005) crystals at different temperatures is shown in Fig. 7. It is determined that the frequency dependence of the imaginary part of the complex dielectric permittivity is of a relaxation nature.

Fig. 8 shows the comparison of the frequency dependence of the *tanδ* of the $TlGaSe_2$ (curve 1) and the $TlGa_{0.995}Er_{0.005}Se_2$ (curve 2) crystals. This dependence is characterized by hyperbolic reduction, which is associated with a loss of conductivity. The increase of *tanδ* at high frequencies indicates the presence of relaxation losses. Compared to $TlGaSe_2$, the value of the *tanδ* of $TlGa_{0.995}Er_{0.005}Se_2$ crystal is significantly increased.

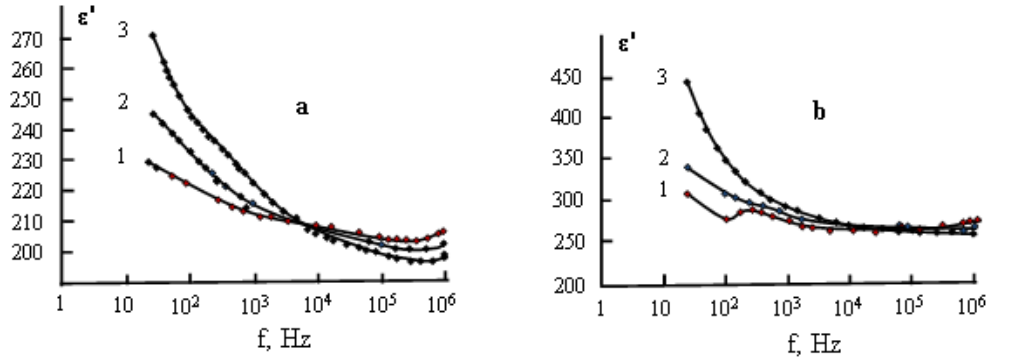

Fig. 6. Frequency dependences of the real part of the complex dielectric permittivity of $TlGa_{1-x}Er_xSe_2$ crystals: a) x=0; b) x=0.005. T: 1-180 K, 2-230 K, 3-300 K.

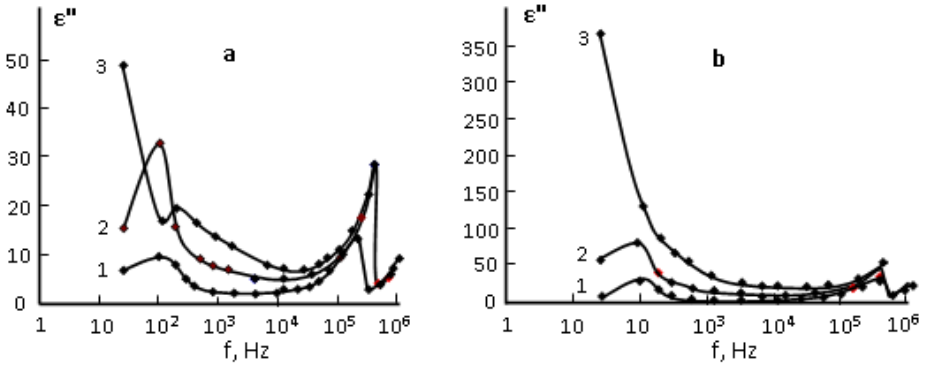

Fig. 7. Frequency dependences of the imaginary part of the complex dielectric permittivity of $TlGa_{1-x}Er_xSe_2$ crystals:
a) x=0; b) x=0.005. T: 1-180 K, 2-230 K, 3-300 K.

We also investigated the frequency dependence of the ac-conductivity in $TlGa_{1-x}Er_xSe_2$ (x=0; 0.005) crystals (Fig. 9).

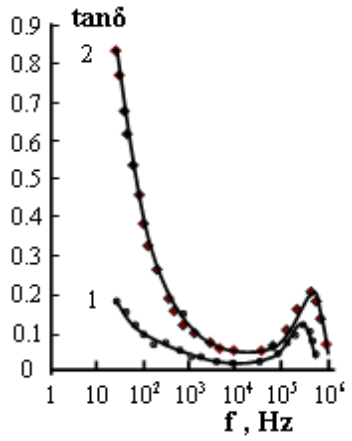

Fig. 8. Frequency dependences of dielectric loss tangent in $TlGa_{1-x}Er_xSe_2$ crystals: 1) x=0; 2) x=0.005, T = 300 K

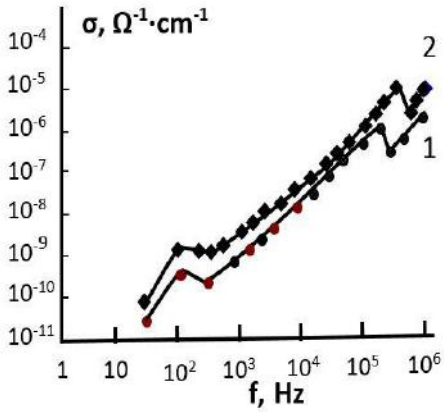

Fig. 9. Frequency dependence of the conductivity of $TlGa_{1-x}Er_xSe_2$ crystals: 1) x = 0, 2) x=0.005. T-180 K.

The σ_{ac} value for $TlGa_{0.995}Er_{0.005}Se_2$ solid solution is higher than for $TlGaSe_2$ crystal.

The dependence curves $\sigma_{ac}(f)$ of $TlGa_{1-x}Er_xSe_2$ (x=0; 0.005) solid solution are observed in 3 parts: in the first case, $\sigma_{ac} \sim f^{0.6}$ was observed and then increased to $\sigma_{ac} \sim f^{0.8}$ (10^2 -10^4 Hz). Then, when the frequency was increased to 1 MHz, it was replaced by $\sigma_{ac} \sim f^{1,2}$. The fact that we obtain it from the law of $\sigma_{ac} \sim f^{0.8}$ indicates that there is the hopping conductivity in localized states near the Fermi level.

Table 4 shows the calculated parameters for $TlGa_{1-x}Er_xSe_2$ (x=0; 0.005) ($f = 10^4$ Hz) within the Mott approximation of solid solutions. The dependence of $\sigma_{ac} \sim f^{0.8}$ on the studied crystals at 10^2-10^4 Hz frequencies is observed. The density of localized states (N_F) near the Fermi level for the $TlGa_{1-x}Er_xSe_2$ (x=0; 0.005) solid solutions is calculated according to Mott's theory [17] by the formula:

$$\sigma_{ac}(f) = \frac{\pi^3}{96} e^2 kT N_F^2 a^5 f \left[\ln\left(\frac{\nu_{ph}}{f}\right)\right]^4$$

Here e is the elementary charge, k - Bolsman constant, N_F - density of states near the Fermi level, $a = 1/\alpha$ is the localization radius, $\psi \sim e^{-\alpha r}$ is the wave function of the localized charge carriers; ν_{ph} - phonon frequency. When calculating the density of localized states near the Fermi level, the localization radius a = 34 Å was taken for the $TlGaSe_2$ crystal [15]. The value of the density of localized states (N_F) near the Fermi level calculated by Mott's theory is given in the table 1. When the temperature increases for 0.5 % Er samples, the value of the density of localized states near the Fermi level increases ($N_F = 2.23\times10^{18}$ $eV^{-1}cm^{-3}$ when x = 0, and $N_F = 3.08\times10^{18}$ $eV^{-1}cm^{-3}$ when x=0.005). According to the theory of hopping conductivity in the alternating current, the hopping distance (R) is determined by the expression [17]:

$$R = \frac{1}{2\alpha}\ln\left(\frac{\nu_{ph}}{f}\right)$$

The value of the R and E_a was calculated for $TlGa_{1-x}Er_xSe_2$ crystals: R=312 Å at 10^4 Hz [17]:

$$\Delta E = \frac{3}{2\pi R^3 N_F}\ , \quad E_a = \left(\frac{(kT)^3}{N_F a^3}\right)^{\frac{1}{4}}$$

According to this expression, the energy spread ΔE of the states localized near the Fermi level in $TlGa_{1-x}Er_xSe_2$ can be estimated.

Table 4 shows that the increase in temperature and the presence of Er in $TlGaSe_2$ increases the density of localized states near the Fermi level, narrows the energy spread ΔE, and changes the value of concentration on local levels.

Table 4.

The parameters of localized states in $TlGa_{1-x}Er_xSe_2$ solid solutions obtained from high-frequency dielectric measurements.

Crystal composition $TlGa_{1-x}Er_xSe_2$	T, K	N_F, $eV^{-1}cm^{-3}$	ΔE, meV	N_t, cm^{-3}	E_a, eV
x = 0	180	$1.54\cdot10^{18}$	10	$1.54\cdot10^{16}$	0.088
	230	$1.76\cdot10^{18}$	9	$1.56\cdot10^{16}$	0.102
	300	$2.23\cdot10^{18}$	7	$1.57\cdot10^{16}$	0.118
x = 0.005	180	$2.48\cdot10^{18}$	6.7	$1.66\cdot10^{16}$	0.078
	230	$2.58\cdot10^{18}$	6.3	$1.62\cdot10^{16}$	0.093
	300	$3.08\cdot10^{18}$	5	$1.54\cdot10^{16}$	0.109

The analysis of the absorption spectra of $TlGa_{1-x}Er_xSe_2$ crystals, namely, the dependence of $(\alpha\hbar\omega)^2$ on the photon energy $\hbar\omega$, made it possible to determine the energies of direct transitions in the studied crystals, and, consequently, their band gap E_g. In the temperature range from 77 to 300 K, the temperature dependences of the band gap of the studied solid solutions were constructed (Fig. 10).

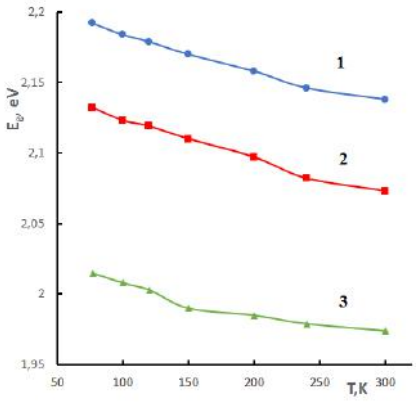

Fig. 10. Temperature dependences of the band gap of $TlGa_{1-x}Er_xSe_2$ single crystals. 1 - x = 0; 2 - x = 0.001; 3 - x = 0.005.

The experiment showed that the following differences are observed in the structure of the absorption edge of $TlGaSe_2$ single crystals and $TlGa_{1-x}Er_xSe_2$ solid solutions: at low temperatures, the absorption band associated with the formation of an exciton near the direct edge cannot be detected in solid solutions; the absorption coefficient in $TlGa_{1-x}Er_xSe_2$ is noticeably higher than in $TlGaSe_2$. The average temperature coefficient of the band gap dE_g/dT in the temperature range 77-300K for $TlGaSe_2$ and $TlGa_{0.999}Er_{0.001}Se_2$ is $-2.4\cdot10^{-4}$ eV/K, and for $TlGa_{0.995}Er_{0.005}Se_2$ is $-1.9\cdot10^{-4}$ eV/K. The long-wavelength band gap shift for $TlGa_{0.999}Er_{0.001}Se_2$ relative to $TlGaSe_2$ at T=77 K is 60 meV, and for $TlGa_{0.995}Er_{0.005}Se_2$ it is 177meV.

4. CONCLUSIONS

The electrical conductivity, dielectric constant, and dielectric loss tangent of the $TlGa_{1-x}Er_xSe_2$ solid solution in an alternating electric field are investigated. In the crystals studied, the change in the dielectric constant as a function of temperature (150–300 K) at low frequencies is associated with the presence of relaxation polarization. $\sigma_{ac}(f)$ in $TlGa_{1-x}Er_xSe_2$ (x =0; 0.005) crystals, at frequencies of 10^2-10^4Hz obeys the law $\sigma_{ac} \sim f^{0.8}$. This indicates the presence of a hopping mechanism of charge transfer in states localized near the Fermi level. Doping the $TlGaSe_2$ crystal with erbium increases the density of states localized near the Fermi level and reduces their spread. An increase in the erbium concentration in $TlGa_{1-x}Er_xSe_2$ solid solutions leads to a decrease in the band gap and its temperature coefficient modulus.

[1] *D. Müller and H. Hahn:* Zur Struktur des $TlGaSe_2$. Z. Anorg. Allg. Chem. 438(1), 1978, 258-272.

[2] E.*M. Kerimova, S.N. Mustafaeva, D.A. Huseinova.* Hard radiation detectors on A^3B^6-based semiconductors and their complex analogues. Proceedings of Eurasia Conf. on nuclear science and its appl., Turkey, 2000, 394.

[3] *S. Johnsen, Z. Liu, J.A. Peters, J.-H. Song, S.C. Peter, C.D. Malliakas, N.K. Cho, H. Jin, A.J. Freeman, B.W. Wessels, M.G. Kanatzidis.* Chem. Mater. 23, 2011, 3120-3128.

[4] *E.M. Kerimova.* Crystal physics of low-dimensional chalcogenides. Baku, Elm, 2012.

[5] *S. Yang, M. Wu, H. Wang, H. Cai, L. Huang, C. Jiang, S. Tongay.* Ultrathin ternary semiconductor $TlGaSe_2$ phototransistors with broad-spectral response. 2D Mater, 4(3), 2017, S1-S6.

[6] *S.N. Mustafaeva, V.A. Aliyev, M.M. Asadov.* Physics of the Solid State, 40, 1998, 41-44.

[7] *S.N. Mustafaeva.* Journal of Radio Electronics, 5, 2008, 1-11.

[8] *A.U. Sheleg, K.V. Iodkovskaya, N.F. Kurilovich.* Physics of the Solid State, 40(7), 1998, 1328-1331.

[9] *S.N. Mustafaeva, M.M. Asadov, A.A. Ismayilov.* Applied Physics 3, 2012, 19-23.

[10] *A.Cengiz, Y.M. Chumakov, M. Erdem, Y. Şale, F.A. Mikailzade, M-H.Y. Seyidov.* Origin of the optical absorption of $TlGaSe_2$ layered semiconductor in the visible range. Semicond. Sci. Technol. 33, 2018, 075019.

[11] *L.Yu Kharkhalisa, K.E. Glukhova, T.Ya Babuka, M.V. Liakha.* Phase Transitions. A Multinational Journal, 2019, 92(5).

[12] *A.M. Panich.* J. Phys.: Condensed Matter, 20 (29), 2008, 293202/1-42.

[13] *A.U. Sheleg, V.V. Shevtsova, V.G. Hurtavoy, S.N. Mustafaeva, E.M. Kerimova.* Low Temperature X-Ray Investigations of $TlInS_2$, $TlGaS_2$ and $TlGaSe_2$ Single Crystals. Surface. X-ray, synchrotron and neutron studies. 11, 2013, 39–42.

[14] *A.Say, D. Adamenko, O. Gomonnai, I. Roman, I. Martynyuk-Lototska, R. Vlokh.* Phase Transitions. A Multinational Journal, 2019, 92(9).

[15] *S.N. Mustafaeva, M.M. Asadov, E.M. Kerimova.* Physics of the Solid State, 55(12), 2013, 2466-2470.

[16] *H.D. Hochheimer, E. Gmelin, W. Bauhofer, et al.* Z. Phys. B. Condens. Matter, 73, 1988, 257-263.

[17] *N.F. Mott, E.A. Davis.* Electronic Processes in Non-Crystalline Materials. Clarendon, Oxford, 1971.

Received: 02.06.2021